THE JOURNAL OF BIOLOGICAL CHEMISTRY VOL. 285, NO. 18, pp. 13550–13560, April 30, 2010

Arabidopsis AtSerpin1, Crystal Structure and *in Vivo* Interaction with Its Target Protease RESPONSIVE TO DESICCATION-21 (RD21)*[S]

Received for publication, December 15, 2009, and in revised form, January 25, 2010 Published, JBC Papers in Press, February 24, 2010, DOI 10.1074/jbc.M109.095075

Nardy Lampl[‡1], Ofra Budai-Hadrian[‡1], Olga Davydov[‡], Tom V. Joss[§], Stephen J. Harrop[¶], Paul M. G. Curmi[¶‖], Thomas H. Roberts[§], and Robert Fluhr[‡2]

From the [‡]Department of Plant Sciences, Weizmann Institute of Science, Rehovot 76100, Israel, the [§]Department of Chemistry and Biomolecular Sciences, Macquarie University North Ryde, Sydney, New South Wales 2109, Australia, the [¶]School of Physics, University of New South Wales, Sydney, New South Wales 2052, Australia, and the [‖]St. Vincent's Centre for Applied Medical Research, St. Vincent's Hospital, Sydney, New South Wales 2010, Australia

In animals, protease inhibitors of the serpin family are associated with many physiological processes, including blood coagulation and innate immunity. Serpins feature a reactive center loop (RCL), which displays a protease target sequence as a bait. RCL cleavage results in an irreversible, covalent serpin-protease complex. AtSerpin1 is an *Arabidopsis* protease inhibitor that is expressed ubiquitously throughout the plant. The x-ray crystal structure of recombinant AtSerpin1 in its native stressed conformation was determined at 2.2 Å. The electrostatic surface potential below the RCL was found to be highly positive, whereas the breach region critical for RCL insertion is an unusually open structure. AtSerpin1 accumulates in plants as a full-length and a cleaved form. Fractionation of seedling extracts by nonreducing SDS-PAGE revealed the presence of an additional slower migrating complex that was absent when leaves were treated with the specific cysteine protease inhibitor L-*trans*-epoxysuccinyl-L-leucylamido (4-guanidino)butane. Significantly, RESPONSIVE TO DESICCATION-21 (RD21) was the major protease labeled with the L-*trans*-epoxysuccinyl-L-leucylamido (4-guanidino)butane derivative DCG-04 in wild type extracts but not in extracts of mutant plants constitutively overexpressing *AtSerpin1*, indicating competition. Fractionation by nonreducing SDS-PAGE followed by immunoblotting with RD21-specific antibody revealed that the protease accumulated both as a free enzyme and in a complex with AtSerpin1. Importantly, both RD21 and AtSerpin1 knock-out mutants lacked the serpin-protease complex. The results establish that the major *Arabidopsis* plant serpin interacts with RD21. This is the first report of the structure and *in vivo* interaction of a plant serpin with its target protease.

Protease cascades are prominent mediators of rapid physiological responses in animals, playing a role in cellular immunity, blood clotting, and development. The proteolytic specificity of the serine and cysteine proteases involved dictates the fidelity of these reactions. The serpins are an important group of proteins that curb the activity of these cascades through specific irreversible inhibition of the proteases. For example, in *Drosophila*, the necrotic (*nec*) gene encodes a protease inhibitor of the serpin family. Necrotic protein controls a proteolytic cascade that activates the innate immune response to fungal and Gram-positive bacterial infections (1). In *nec* null mutants, Toll-mediated immune responses are constitutively activated, even in the absence of infection, implying that *Nec* continually restrains this immune response. As opposed to other types of protease inhibitors, serpins offer both an irreversible and tunable type of inhibition (reviewed in Ref. 2). In their native conformation, serpins are in a stressed (spring-loaded) state with a solvent-exposed reactive center loop (RCL).[3] Specific residues of the RCL are precisely accommodated by the target protease active site. Upon cleavage of the serpin peptide bond linking the P1 and P1′ residues (3), an ester bond forms between the protease active site serine (or cysteine) and the carbonyl carbon of the P1 residue. This is followed by a dramatic and irreversible conformational change in the residual part of the loop; the cleaved RCL snaps as an extra strand into β-sheet A between the breach formed by strands s5A and s3A, dragging with it the covalently linked protease. The resulting compression destabilizes the protease, which cannot then affect hydrolysis or detachment, to form a stable, covalent complex (4, 5). Evolution has taken advantage of the high specificity of these suicide-substrate inhibitors, allowing serpins to become the predominant protease inhibitors in animal signaling pathways. In humans, serpins belong to a large multigene family in which loss- or gain-of-function mutations lead to compromised innate immune responses, dementia, thrombosis, and other diseases (6–8).

Plant serpins are potent inhibitors of a range of mammalian serine proteases *in vitro*, and at least seven serpin genes are expressed in *Arabidopsis* (reviewed in Ref. 9). Serpins from

* This work was supported by Grant 1306/06 (to R. F.) by the Israel Science Foundation, Macquarie University funding (to T. H. R.), and Australian Research Council funding (to P. M. G. C.).

[S] The on-line version of this article (available at http://www.jbc.org) contains supplemental Table 1 and Figs. S1–S3.

The atomic coordinates and structure factors (code 3LE2) have been deposited in the Protein Data Bank, Research Collaboratory for Structural Bioinformatics, Rutgers University, New Brunswick, NJ (http://www.rcsb.org/).

[1] Both authors contributed equally to this work.

[2] To whom correspondence should be addressed. Tel.: 972-8-9342175; Fax: 972-8-9344181; E-mail: robert.fluhr@weizmann.ac.il.

[3] The abbreviations used are: RCL, reactive center loop; E-64, L-*trans*-epoxysuccinyl-L-leucylamido (4-guanidino)butane; DCG-04, biotinylated derivative of L-*trans*-epoxysuccinyl-L-leucylamido (4-guanidino)butane; HA, hemagglutinin; VPE, vacuolar processing enzyme; ko, knock-out; ER, endoplasmic reticulum.

cereal grains are irreversible inhibitors of serine proteases with distinct inhibitory specificity (10, 11). The majority of inhibitory serpins from wheat and rye grain contain motifs within the RCL that resemble the glutamine-rich repeats of grain storage proteins, suggesting a function in the protection of storage protein degradation by exogenous proteases (12, 13). In addition, the differential expression of serpins in barley grain suggested a function in seed survival within the herbivore digestive tract (14). Similarly, *Cucurbita maxima* phloem serpin-1 (CmPS-1) was shown to have anti-elastase-like specificity. A related serpin from *Cucurbita sativa,* CsPS-1, was localized exclusively to sieve elements (15), where it is thought to play a role in defense against herbivores (16). Interestingly, a correlation was found between a developmentally regulated increase in the amount of CmPS-1 and the reduced ability of the aphid, *Myzus persicae*, to survive. However, in that case, experiments with purified phloem CmPS-1 added to the aphid diet failed to demonstrate a direct effect on survival (17). Recently, an *Arabidopsis* serpin, *AtSerpin1* (At1g47710), was reported to interact *in vitro* with the endogenous plant cysteine protease metacaspase 9 (AtMC9) (18). Evidence has also been found for participation of two other *Arabidopsis* serpins, *AtSRP2* (At2g14540) and *AtSRP3* (At1g64030), in growth responses to plant exposure to the DNA-alkylating agent methyl methanesulfonate (19).

Serpins in animals are mostly associated with inhibition of serine proteases of the chymotrypsin family (clan PA, family S1; MEROPS). In plants, the proteases of this family are absent (12), but several other families of distinct protease clans (including caspase-like, papain-like, and subtilisin-like proteases) have been shown to play a role in general plant defense responses (20, 21). Cysteine proteases have been shown to be associated with general stress effects and the hypersensitive response (20, 22, 23). Senescence stress induces the expression of the cysteine vacuolar proteases, vacuolar processing enzyme-γ (VPEγ) and RD21 (24), and the processing of RD21 into the mature active form (25). The application of cysteine-specific proteolytic inhibitors (26) or overexpression of the natural cysteine protease inhibitor cystatin (27, 28) delays stress-induced cell death. Similarly, plant metacaspases can activate apoptosis-like cell death in yeast (29), play a role in self-incompatibility-induced programmed cell death in pollen (30) and participate in cell death triggered by UVC and H_2O_2 in protoplasts (31). Caspase-specific peptide inhibitors abolished pathogen promotion of programmed cell death in plant cells (32–34). Although plant protease activity plays an important role in defense and developmental processes, less is known of its control, and it is unknown whether serpins can interact *in planta* with any of these potential candidates.

Subtle differences in otherwise conserved protein structures give different serpins special properties, such as modulation of their inhibitory activity by binding to other proteins, nucleic acids, and small molecules (35). Phylogenetic analysis of all known serpins (36, 37) and of plant serpins alone (9) has shown that plant serpins tend to cluster in a species-specific manner; hence, comparative phylogeny is of limited use for surmising their functionality. There are no plant serpin structures to compare with the large number available from animals and prokaryotes to allow identification of any special features of the Clade P (plant) serpins. We wished to determine the structure of AtSerpin1, to compare it with known animal serpins that have the ability to inhibit serine and/or cysteine proteases, and to establish the protease target of AtSerpin1 by examining gain- and loss-of-function serpin mutants of *Arabidopsis*.

Here, we present the x-ray crystal structure of AtSerpin1 in the native, metastable stressed state, revealing several novel and plant-specific features. We show that AtSerpin1 can form SDS-stable complexes in a manner that is sensitive to the addition of the potent cysteine protease inhibitor, E-64. With the help of knock-out mutants, overexpression lines, and specific antibodies, we establish that the major AtSerpin1 target is the RESPONSIVE TO DESICCATION-21 cysteine protease RD21.

EXPERIMENTAL PROCEDURES

Determination of AtSerpin1 Structure—The full-length *AtSerpin1* cDNA was obtained via The *Arabidopsis* Information Resource and was cloned into a pET100/D-TOPO expression vector (Invitrogen) whereby the protein was equipped with an N-terminal His_6 tag. The vector insert was sequenced to check for cloning errors. Constructs were transformed into *Escherichia coli* BL21(DE3) (Novagen). Purification of soluble recombinant His-tagged protein was performed through the sequential use of nickel-nitrilotriacetic acid affinity chromatography and desalting. Polypeptide identity was validated by SDS-PAGE (supplemental Fig. S1*A*) and tryptic digestion combined with mass spectrometry (supplemental Fig. S1*B*). Initial crystallization screens were performed with 480 conditions in a 96-well format with 400-nl drops using commercial Qiagen screens. In initial screening, crystals were observed after 48 h in over 15 conditions, predominantly with $(NH_4)_2SO_4$- and polyethylene glycol/ion-based buffers. Optimization screens were performed in 24-well format with 2-μl drops. Robust 250-μm cube crystals were obtained by vapor diffusion after 6 days using a well solution of 2 M ammonium sulfate plus 0.2 M sodium acetate. Crystals initially diffracted to 4 Å, which was improved to 2.8 Å on a rotating anode source by cryo-annealing the crystals (38). The space group was $P4_322$, and the dimensions of the unit cell were 54.20 × 54.20 × 299.34 Å.

Crystals were cryoprotected by the addition of glycerol (10–15%), and diffraction data were collected at 100 K both in-house (2.8 Å resolution using a Nonius FR591 rotating anode x-ray generator with Mar345dtb image plate detector plus confocal mirrors) and at 2.2 Å resolution using the Advanced Photon Source 23-ID-B at the Argonne National Laboratory (see supplemental Table 1). Data reduction was carried out using the programs MOSFLM and SCALA from the CCP4 suite (39). The structure was solved by molecular replacement using the program PHASER (40) with the structure of human plasminogen activator inhibitor-2 as a search model (Protein Data Bank accession code 1BY7 (41)). Model rebuilding was carried out using crystallographic object-oriented toolkit (COOT) (42), and the structure was refined using the PHENIX suite of programs (43). The crystals contained one AtSerpin1 molecule per asymmetric unit. Clear electron density was observed for all residues of AtSerpin1, including the RCL plus two residues from the N-terminal purification tag. Ordered solvent mole-

cules included 259 water molecules, 2 acetate ions, and 1 glycerol from the cryoprotectant. The final *R*-factor was 0.173 with an *R*-free of 0.236 (see supplemental Table 1). The coordinates and structure factors have been deposited in the Protein Data Bank (accession code 3LE2).

Vector Construction, Plant Transformation, and Mutant Lines—AtSerpin1 expressed sequence tag clone (accession number R65473) was received from the *Arabidopsis* Biological Resource Center (Ohio State University). A hemagglutinin (HA) epitope-tagged transgene, AtSerpin1-HA, was constructed by combining the respective forward oligonucleotide 5′-TGCTCTAGAATGGACGTGCGTGAATCAATC-3′ with the reverse oligonucleotide 5′-AGGCCCGGGATGCAACGGATCAACAACTTG-3′. The clone was fused upstream to three repeats of the HA epitope (YPYDVPDYA) in pPZP111 (44) under the control of the 35S promoter from the cauliflower mosaic virus by XbaI-SmaI and used to transform *Agrobacterium tumefaciens* strain EHA105. An *AtSerpin1* insertion line was identified in the SALK tDNA collections (45) as SALK_075994. The tDNA is inserted at the C-terminal region of the gene at nucleotide 1694 in the second exon. The AtSerpin1 full-length expressed sequence tag clone was cloned by SalI-HindIII digestion into the PQE-30 expression vector (Qiagen, Hilden, Germany) into a position that was downstream from the His tag and used to raise polyclonal antibodies in guinea pigs.

Plant Growth Conditions, Treatments, Immunoassay, and Protein Sequencing—*Arabidopsis thaliana* ecotype Col-0 plants were grown under white light in a 16-h light/8-h dark cycle at 21 °C. Antibodies anti-HA.11 were obtained from Babco, Richmond, CA). Immunopurification of AtSerpin1 from total protein extract of AtSerpin1-HA leaves was carried out with covalently linked AtSerpin1 using the Seize X protein A immunoprecipitation kit (Pierce). The fractionated proteins were subjected to trypsin digestion for amino acid determination using liquid chromatography-nanospray tandem mass spectrometry. For E-64 inhibition analysis, overexpression AtSerpin1-HA plants were grown on solid agar medium that contained B5 Gamborg's nutrients in 0.8% (w/v) phytoagar (Invitrogen) in controlled environment chambers at 21 °C under a 16-h light regime. Experiments were performed on 14-day-old seedlings, which were gently brush-spread with different concentrations (10, 50, and 100 μg) of E-64 (E64c, Cayman Chemical, Ann Arbor, MI). After 30 min, whole plants were extracted with extraction buffer (20 mM Tris, pH 8.0, 1 mM EDTA, and 50 mM NaCl), followed by centrifugation (15 min, 17,000 × *g*). Gel fractionation was carried out on 10% SDS-PAGE. For reducing gels, the Laemmli loading buffer contained 1% (v/v) β-mercaptoethanol as reducing agent, whereas the loading buffer for nonreducing gels did not contain any reducing agent. Fractionated proteins were transferred onto polyvinylidene fluoride membrane (Bio-Rad). The membrane was developed with AtSerpin1 antibodies (1:1,000) and secondary anti-guinea pig horseradish peroxidase (1:3,000).

Protease Profiling—Cysteine proteases were labeled with DCG-04 as described in Greenbaum *et al.* (51). Proteins of 14-day-old seedlings were extracted by grinding the whole plants with a mortar and pestle and mixing with extraction buffer (20 mM Tris, pH 8.0, 1 mM EDTA and 50 mM NaCl), followed by centrifugation (15 min, 17,000 × *g*). The extract (0.3 mg) was labeled in 0.125-ml total volume, containing 50 mM sodium acetate buffer, pH 6, 10 mM dithiothreitol, and 2 μM DCG-04. Control samples contained 0.2 mM E-64. Labeling was done with gentle shaking for 3 h at room temperature. Biotinylated proteins were separated on reducing 10% SDS gels and detected with streptavidin-horseradish peroxidase (1:3,000, The Jackson Laboratories). The same membranes were reblotted with AtSerpin1 antibodies (1:1,000), secondary anti-guinea pig horseradish peroxidase (1:3,000), RD21 antibodies (1:1,000), and secondary anti-rabbit horseradish peroxidase (1:3,000).

In Vitro Binding—Plants of 14-day-old seedlings, AtSerpin1-ko and RD21-ko, were extracted in binding buffer (50 mM sodium acetate, pH 6.0, 1 mM EDTA) and incubated at room temperature for 30 min with 3 mM dithiothreitol and in the presence or absence of recombinant AtSerpin1. Samples were then analyzed by nonreducing SDS-PAGE and immunoblotting with anti-RD21 and AtSerpin1 antibodies.

RESULTS

X-ray Crystal Structure of AtSerpin1 Highlights Conserved and Plant-specific Structural Features—The crystal structure of AtSerpin1 was determined to 2.2 Å resolution (Fig. 1 and see supplemental Table 1). Clear electron density was observed for all residues in the serpin sequence, including the RCL. The serpin is in the native, stressed state. The RCL is stabilized by crystallographic packing and by a glycerol molecule from the cryoprotectant. Overall, the AtSerpin1 structure resembles those of canonical serpins comprising three conserved β-sheets (conventionally labeled sA, sB, and sC; colored *yellow, cyan,* and *magenta*, respectively; Fig. 1*A*) and nine conserved α-helices (labeled hA through hI in sequence order, colored *red*). An additional helix is seen in the RCL, as well as three single-turn helices (one prior to s4C below the RCL, which is seen in other serpins, and two short helices at the base of the serpin following hI; see Fig. 1*A*).

There are several features that distinguish the AtSerpin1 structure. The loop joining β-strands s2B and s3B is relatively long (Fig. 1*A*), containing a plant-specific motif between Tyr-225 (the conserved breach tyrosine) and the hydrophobic core amino acid Phe-234 (see Pfam alignment (46)). An alignment of 67 expressed plant serpin sequences (9) shows that the motif Y*XXG*X*D*X*R*X*F* is present in 54 of these sequences, with an additional eight sequences containing conservative variations of the motif. This motif is not seen in non-plant serpins, with other eukaryotic serpins usually containing three to four residues between the breach tyrosine and the core hydrophobic residue (as opposed to eight residues in plants). In the structure of AtSerpin1, the conserved Asp-230 and Arg-232 of this plant-specific motif form a network of hydrogen bonds that links the s2B-s3B junction to the loop connecting helix hD and β-strand s2A (Fig. 1, *A* and *C*). These interactions stabilize this loop region, which is otherwise disordered in many other serpin structures.

Another distinguishing feature of AtSerpin1 is the presence of a β-bulge in strand s2C (Fig. 1, *A* and *D*). The residues in this

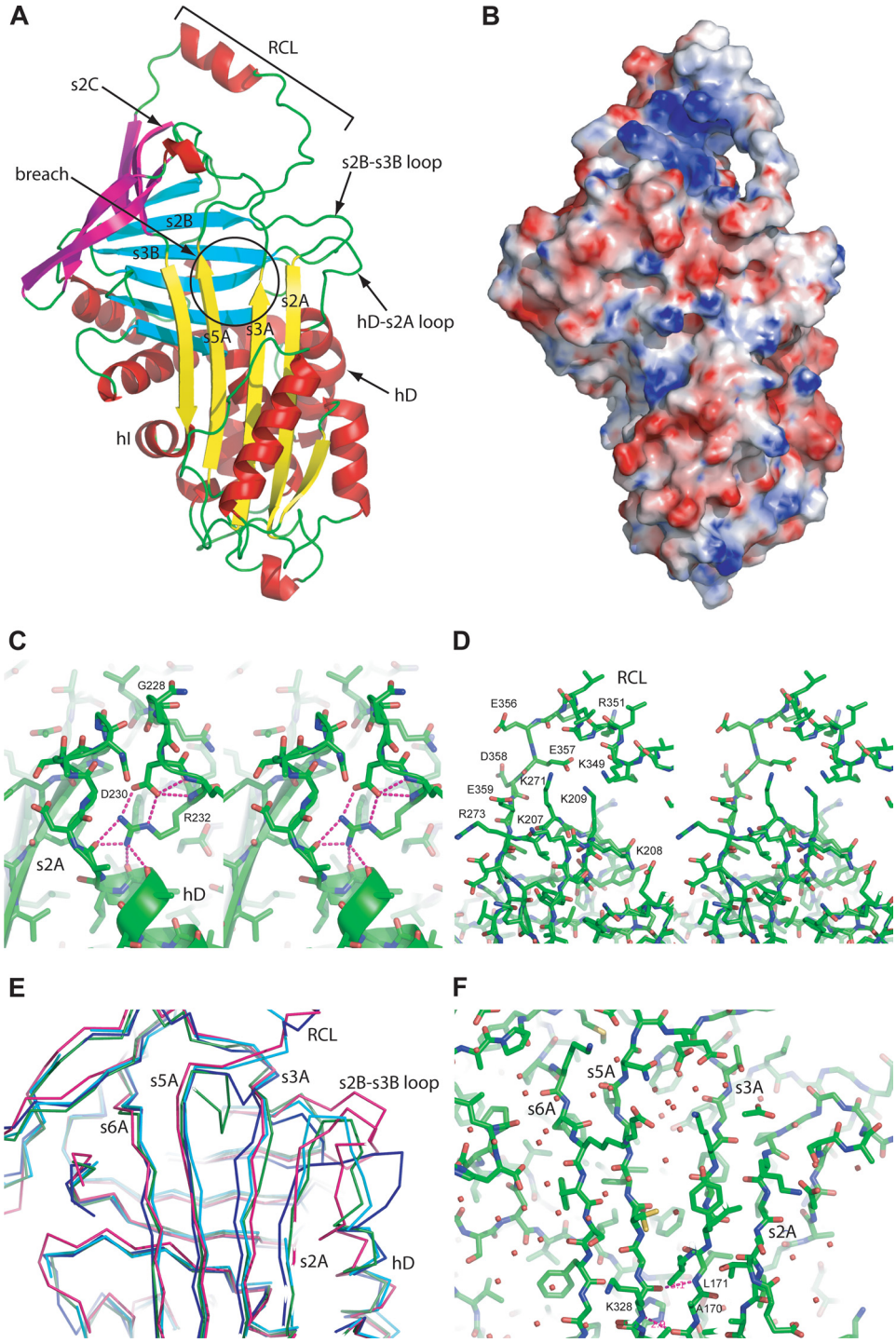

FIGURE 1. **Structure of AtSerpin1.** *A,* ribbon diagram showing the structure of AtSerpin1. *B,* molecular surface of AtSerpin1 showing the electrostatic potential. *Blue* indicates positive, and *red* indicates negative potential. *C,* stereo illustrations of the loop region between β-strands s2B and s3B in the proximity of helix hD. Residues that make up the loop region Gly-228, Asp-230, and Arg-232 are indicated. Asp-230 and Arg-232 form a charged structure that stabilizes the loop between helix hD and β-strand s2A with a network of hydrogen bonds as illustrated. *D,* stereo illustrations of AtSerpin1 showing the charged residues at the top of β-sheet sC and the RCL region. Basic residues in this sheet are indicated as follows: Lys-207, Lys-208, Lys-209, Arg-273, and Lys-271. The reactive center cleavage site (P4–P8′, ^{348}IKLRGLLMEEDE^{359}) is positioned above the β-sheet. It consists of hydrophobic and basic residues (Lys-349 and Arg-351) in its N terminus and acidic residues at its C terminus (Glu-356, Glu-357, Asp-358, and Glu-359). *E,* overlay of the breach region of selected serpins. The breach of stressed state serpins and a serpin with a partially inserted RCL is compared. AtSerpin1, *magenta*; α_1-antitrypsin, *blue*; protein C inhibitor, *cyan*; SerpinA3n with a partially inserted RCL structure, *green*. *F,* structure of the breach region of AtSerpin1. The breach between the backbone of s5A and s3A shows hydrogen bonding (*magenta dashed lines*) at the S10 site. The remainder of the breach is filled with ordered water molecules (*red spheres*), which are hydrogen bonded to the backbone.

strand together with additional basic residues in strand s3C project positive charges toward the RCL (Fig. 1, *B* and *D*). Because of the clustering of basic residues in β-sheet sC, the resultant electrostatic potential map for AtSerpin1 has a striking positively charged surface at the top of the serpin body surface (β-sheet sC) and directly underneath the RCL (*blue patch* at the *top* of Fig. 1*B*). This positive potential is largely due to Lys-209 and Lys-271, and the former is common to plant serpins (present in 44/67 expressed plant serpin sequences), and the latter is less common (lysine or arginine present in 14/67 expressed plant serpin sequences). Interestingly, in AtSerpin1, the RCL itself is also basic between P14 and P4′, but these residues are followed by four acidic residues from P5′ to P8′ (EEDE). This acidic region is unique to AtSerpin1 with the only similar plant serpin being that from *Brassica napus,* which has three acidic residues in this segment.

Breach Is Open in the Native (Stressed State) Structure of AtSerpin1—The breach defines a partial separation at the C-terminal end of β-strands s3A and s5A (Fig. 1*A*) and is thought to facilitate the entry of the cleaved RCL into the serpin body during the stressed-to-relaxed (S→R) state transition. The breach of AtSerpin1 is unusually open for a stressed state structure (Fig. 1*E*) with ordered water molecules bridging between the two β-strands (Fig. 1*F*). Indeed, overlay of AtSerpin1 (*magenta,* Fig. 1*E*) with α_1-antitrypsin (*blue*) accentuates the open nature of the AtSerpin1 breach. It appears to be more similar to the open breach structure of the contrapsin-like protease inhibitor 6, SerpinA3n, which was obtained in the presence of a partially inserted RCL (*green,* Fig. 1*E*). The only other native, stressed state serpin that resembles AtSerpin1 is protein C inhibitor (*cyan,* Fig. 1*E*) where the breach is almost as open as in AtSerpin1. Incidentally, the protein C inhibitor crystal structure has three copies of protein C inhibitor in the

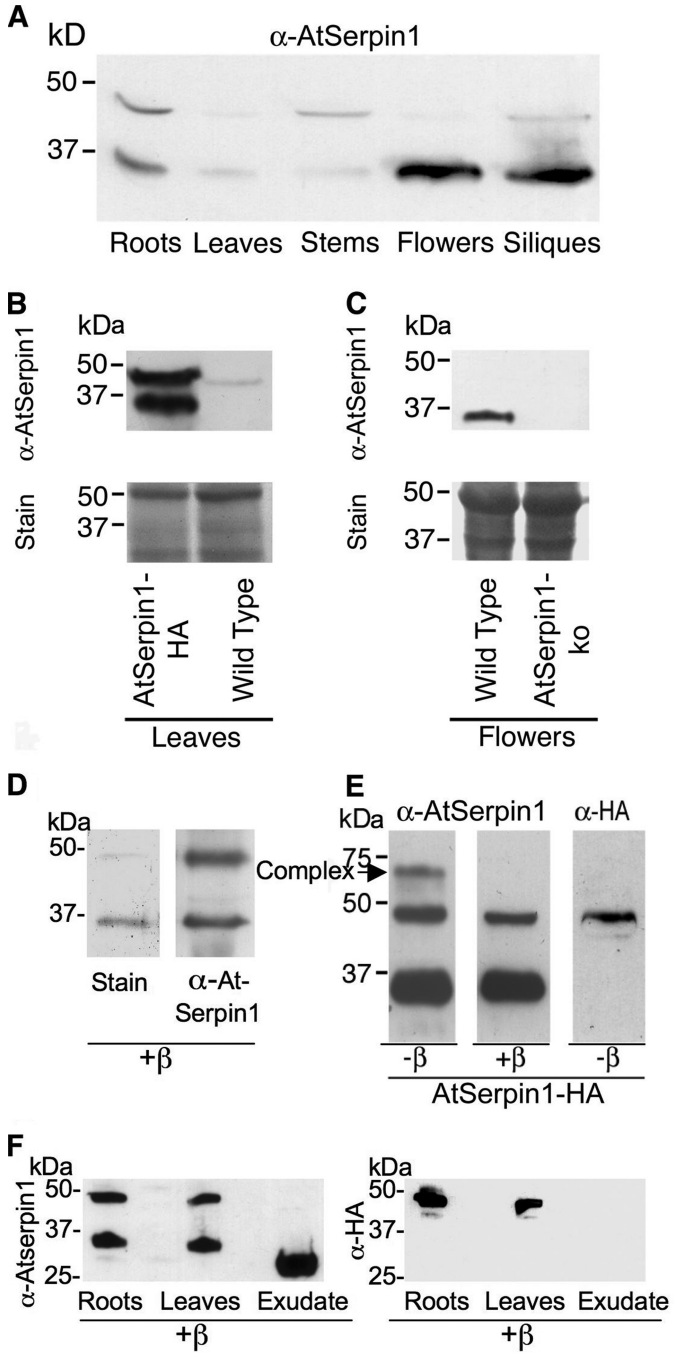

FIGURE 2. **Tissue-specific expression of AtSerpin1.** *A,* immunoblot of AtSerpin1 polypeptide. Total protein was extracted from 3-week-old plant organs for roots and leaves. Extracts of stem, flowers, and siliques were from 8-week-old wild type plants. Equal amounts of protein (150 μg) were loaded on reducing SDS-PAGE, immunoblotted, and developed with α-AtSerpin1 antibody. *B,* immunoblot of leaf extracts from wild type and AtSerpin1-HA line 12.11.8. Equal amounts of protein (30 μg) were loaded on reducing SDS-PAGE and stained with Coomassie stain (*lower panel*) and then immunoblotted and developed with α-AtSerpin1 antibody (*upper panel*). *C,* immunoblot of flower extracts from wild type and AtSerpin1-ko line. Equal amounts of protein (150 μg) were loaded on reducing SDS-PAGE, stained with Coomassie stain (*lower panel*), and then immunoblotted and developed with AtSerpin1 α-antibody (*upper panel*). *D,* immunoprecipitation of AtSerpin1 polypeptide from AtSerpin1-HA plants. The eluate was loaded on reducing SDS-PAGE for Coomassie staining (*left*) and for immunoblot developed with α-AtSerpin1 antibody (*right*). *E,* fractionation of extracts from AtSerpin1-HA plants in reducing and nonreducing gel conditions. Extracts (60 μg) from AtSerpin1-HA plants were fractionated on SDS-PAGE with (+β) or without (−β) the addition of β-mercaptoethanol as reducing agent as described under "Experimental Procedures." Immunoblots were developed with α-AtSerpin1 antibody or α-HA antibody. The *arrow* points to the putative serpin-protease complex. *F,* immunoblot of AtSerpin1 polypeptide. AtSerpin1-HA plants were grown in liquid medium for 2 weeks. Total protein was extracted from roots, leaves, and medium. Extracts (30 μg) were fractionated by reducing SDS-PAGE and immunoblotted with α-AtSerpin1 antibody (*left panel*) or α-HA antibody (*right panel*).

asymmetric unit where, in one molecule, the RCL is partially inserted, although the other two (including chain A, shown here in *cyan*, Fig. 1*E*) have open breach regions.

The open state of the breach region can be quantified by determining the position of the first backbone hydrogen bond between β-strands s3A and s5A. Following standard nomenclature (3), each position between β-strands s3A and s5A is labeled by the number of the RCL residue that would insert at the site were the RCL to be cleaved and inserted to form the relaxed state. For the structure of AtSerpin1, the first hydrogen bond between β-strands s3A and s5A occurs between the N of Leu-171 and the C=O of Lys-328 (Fig. 1*F*), which is the S10 site (the site where residue P10 would reside were AtSerpin1 to be cleaved). In contrast to this, comparison of all other stressed state serpin crystal structures with resolution better than 2.4 Å shows that in most structures the hydrogen bonding pattern between s3A and s5A commences at the S13 site, producing a closed breach. Notwithstanding its special features, the AtSerpin1 structure closely resembles serpins that display protease-specific inhibitory activity.

AtSerpin1 Is Differentially Expressed in Root, Leaf, Flower, and Silique Tissue—The expression of *AtSerpin1* at the mRNA level was recently shown to be constant during seedling development and ubiquitous among mature tissues (19). When the protein level was examined in wild type lines by immunodetection, at least two immunoreactive polypeptides of 43- and 37-kDa apparent size were detected by α-AtSerpin1 antibody in extracts fractionated on reducing SDS-PAGE. Relatively higher levels were detected in flowers and siliques compared with root, stem, and leaf tissue (Fig. 2*A*). In contrast, extracts of flower tissue from a line with a tDNA insertion in the C-terminal part of the gene (see under "Experimental Procedures") did not exhibit cross-reactive polypeptides (AtSerpin1-ko; Fig. 2*C*). This result demonstrates the specificity of the antibody and confirms the tDNA insertion line as a serpin knock-out-type (ko) mutant. Cleavage by a cognate protease at the RCL of AtSerpin1 would yield an ~37-kDa polypeptide, as is detected. To examine AtSerpin1 maturation, the serpin polypeptide was fused at the C terminus to an HA tag under control of the 35S promoter, and overexpression lines were isolated. Transgenic plants expressed high constitutive levels of AtSerpin1-HA in leaves. The expected full-length size of the fusion protein is 45-kDa due to the addition of an HA tag at the C terminus. The processed 37-kDa polypeptides remains the same size as it lacks the C terminus (Fig. 2*B*). The results are shown for AtSerpin1-HA line 12.11.8, and similar results were obtained in independent overexpression lines (data not shown).

Protein extracts of AtSerpin1-HA were immunoprecipitated with α-AtSerpin1 antibody, and the two polypeptides of 45 and 37 kDa were recovered (Fig. 2*D,* Coomassie gel and immunoblot). Mass spectrometry sequencing analysis of the 37-kDa

polypeptide yielded 73% coverage of AtSerpin1, including the N-proximal tryptic peptides such as "ESISLQNQVSMNLAK," but no C-terminal peptides were recovered distal to the predicted RCL region (supplemental Fig. S2). The loss of the C-terminal region in the faster migrating polypeptide can also be deduced by the lack of immunodetection of the C-terminal HA tag in the cleaved 37-kDa polypeptide as shown in Fig. 2, *E* and *F* (*right panels*, α-HA). Thus, the presence of the lower molecular weight polypeptide is consistent with *in vivo* cleavage in the RCL region.

AtSerpin1 Is Targeted to the Secretory Pathway—AtSerpin1 was predicted by some algorithms to contain a secretory signal peptide (supplemental Fig. S2) and thus be targeted to the cell secretory system. In addition, previous work showed extracellular apoplastic accumulation of full-length and processed forms of AtSerpin1 (18). As apoplastic isolation requires vacuum infiltration that can disrupt cell integrity, the possibility of secretion was reexamined by growing AtSerpin1-HA plants in aseptic liquid culture so that root exudate could be monitored. Immunoblots of extracts developed with α-AtSerpin1 antibody revealed 45- and 37-kDa polypeptides in roots and leaves but a 28-kDa polypeptide in the exudate (Fig. 2*F*, *left panel*). When the same immunoblot was developed with anti-HA antibody only the 45-kDa polypeptide was observed (Fig. 2*F*, *right panel*). Thus, the 45-kDa band corresponds to the full-length AtSerpin1-HA fusion polypeptide, and the 37- and 28-kDa band correspond to AtSerpin1-HA from which the HA tag (*i.e.* the C terminus) was cleaved. The presence of processed AtSerpin1 in the exudate implies that AtSerpin1 can be targeted to the secretory pathway.

AtSerpin1 Can Participate in a Quasi-stable Protein Complex, the Formation of Which Is Inhibited by the Specific Cysteine Protease Inhibitor E-64—Some animal serpin-protease complexes migrate as high molecular weight complexes in SDS-PAGE independent of reducing conditions (47–49). We examined whether AtSerpin1 could also form SDS-stable complexes *in vivo*. To this end, protein extracts from the AtSerpin1-HA line were fractionated by reducing and nonreducing SDS-PAGE. Interestingly, the immunoblot developed with α-AtSerpin1 antibody under reducing conditions revealed polypeptides of ~45 and 37 kDa (*lane* +β; Fig. 2*E*). However, fractionation of the same extract under nonreducing conditions revealed an additional slower migrating polypeptide of 60-kDa apparent size (*left lane*, −β; Fig. 2*E*, *arrow*). When this immunoblot was developed with α-HA antibody, only the 45-kDa polypeptide was detected (*right lane*, −β; Fig. 2*E*). The results are consistent with C-terminal processing of the full-length 45-kDa AtSerpin1 polypeptide to yield the 37-kDa product under reducing conditions. The slower migrating polypeptide detected under nonreducing conditions can represent a reductant-sensitive SDS-stable serpin-protease complex. The sensitivity of the complex to a reducing agent may indicate that the protease active site contains a redox-sensitive active cysteine, *i.e.* it is a cysteine-type protease, or that the serpin itself is redox-sensitive. To differentiate between these possibilities, we employed derivatives of inhibitor E-64, an irreversible broad spectrum inhibitor specific for cysteine proteases of the papain family (50). Different concentrations of E-64c, a synthetic ana-

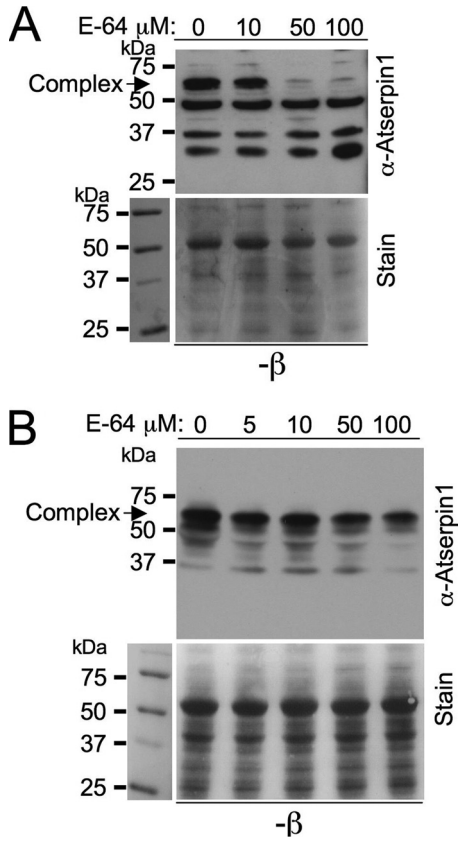

FIGURE 3. **Effect of cysteine protease inhibitor E-64 on AtSerpin1 complex formation *in vivo*.** Leaves or extracts of 2-week-old AtSerpin1-HA plants were treated with different concentrations of E-64 and the extracts fractionated by nonreducing SDS-PAGE. The immunoblots were developed with α-AtSerpin1 antibody. The *lower panels* are loading controls and stained markers. *A*, leaves from 2-week-old plants grown in B5-Gambourg medium were brushed with 0, 10, 50, and 100 μM of E-64c for 30 min, and 80 μg of protein from the extracts was fractionated by nonreducing SDS-PAGE as described under "Experimental Procedures." Immunoblots were developed with α-AtSerpin1 antibody. The *arrow* points to the putative serpin-protease complex. *B*, E-64 at the indicated concentration was incubated with extracts from AtSerpin1-HA leaves for 1 h and fractionated as in *A*.

log of E-64, were applied to leaves of AtSerpin1-HA plants and extracts processed by a nonreducing SDS-PAGE. As shown in Fig. 3*A*, application of E-64c interfered chiefly with the formation of the putative AtSerpin1-protease complex (Fig. 3*A*, *arrow*). The results are consistent with the role of a papain-type protease in AtSerpin1 complex formation. The addition of E-64 to plant extracts *in vitro* had a minor effect on the presence of the preformed complex in the AtSerpin1-HA extract (Fig. 3*B*). Thus, the rapid disappearance of the complex *in vivo* when the formation of new complex was inhibited by E-64 indicates that the complex is subject to rapid turnover as generally occurs for serpin-protease complexes in animal systems.

DCG-04 Detects Cysteine Proteases That Are Protected in the Presence of AtSerpin1-HA—DCG-04 is a biotinylated derivative of E-64 and thus a mechanism-based probe that covalently targets cysteine proteases of the papain family (51). As E-64 was shown to rapidly disrupt *in vivo* serpin complex formation, we wished to identify the putative protease candidates using the DCG-04 probe. In previous work, among the major cross-reacting proteases that were identified in extracts of *Arabidopsis* were XCP2 (xylem cysteine protease 2), *Arabidopsis* Aleurain-

like protease, and RD21, with RD21 migrating at 40- and 30-kDa apparent values (52). Under our conditions for labeling of 2-week-old *Arabidopsis* plants, the major cross-reactivity of streptavidin detected was at 40 and 30 kDa, apparent sizes comparable with the migration pattern of RD21 (Fig. 4, *upper left panel*). Interestingly, in extracts of AtSerpin1-HA plants, less streptavidin cross-reactivity was observed. All labeling was completely abrogated when carried out in the presence of E-64, showing its specificity (Fig. 4, *upper right panel*). The differential labeling by streptavidin may be due to the excess of AtSerpin1 (Fig. 4, *middle panel*) or to the fact that in this line less cysteine protease accumulates. However, when extracts of all the lines were immunoblotted with α-RD21, the accumulation of this protease was found to be similar in all the lines and (as expected) identical to the migration pattern detected by streptavidin. The results show that the presence of excess AtSerpin1 effectively protects the protease from DCG-04 labeling and suggest that RD21 is the protease that is targeted by both DCG-04 and AtSerpin1.

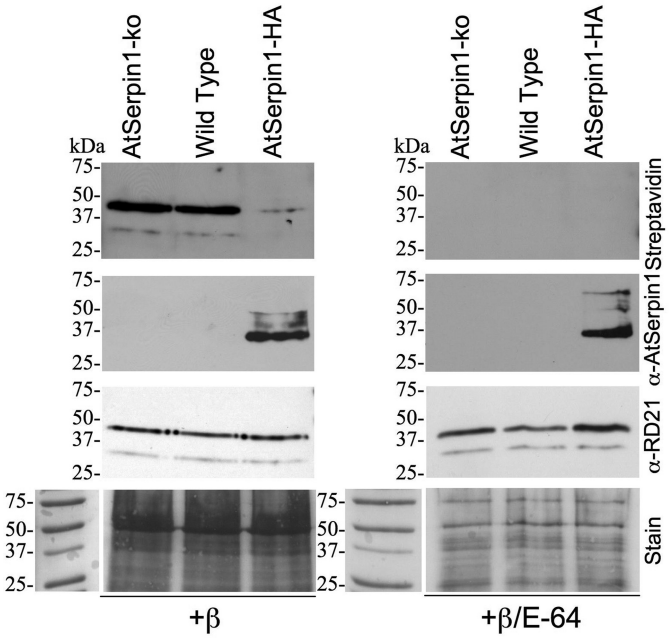

FIGURE 4. **Detection of DCG-04-labeled proteases in plant extracts.** Extracts from 2-week-old AtSerpin1-ko, wild type, and AtSerpin1-HA lines plants were labeled with DCG-04 in the presence or absence of the cysteine protease inhibitor E-64. The extracts (300 μg) were fractionated on reducing SDS gels as described under "Experimental Procedures" and immunoblotted with streptavidin to detect the DCG-04 label (*upper panel*), with α-AtSerpin1 (*middle panel*), and with α-RD21 antibody (*bottom panel*) to detect select polypeptides as indicated. Labeling was done in the absence (*left panels*) or in the presence of 200 μM E-64 (*right panels*). The *lower panels* are loading controls and stained markers.

Presence of RD21 Is Essential for Forming the AtSerpin1 Complex—To determine the contribution of RD21 to the formation of the AtSerpin1 complex, mutant lines deficient in RD21 expression were examined. The tDNA RD21 insertion mutant (*rd21-1*; SALK_090550) has been shown previously to lack RD21 activity (RD21-ko (53)). Although the full-length and processed forms of the AtSerpin1-HA transgene product were readily detected by both nonreducing and reducing SDS-PAGE in AtSerpin1-HA overexpression lines, they were not visible in wild type or (as expected) in AtSerpin1-ko lines (Fig. 5, *A* and *B*). Upon longer exposure, the immunoblot complex could be detected in wild type but not in similarly treated extracts of the RD21-ko line, although in both lines full-length and processed forms of endogenous AtSerpin1 were visible (Fig. 5*C*, *upper panel*). When the immunoblots were re-probed with α-RD21 antibody, the RD21 protease was found to co-migrate with the AtSerpin1-HA complex (Fig. 5*A*, *lower panel*) and was detected as co-migrating with the AtSerpin1 complex in wild type extracts but not RD21-ko extracts. The data show that the endogenous AtSerpin1 and the AtSerpin1-HA transgene products interact with RD21. Interestingly, the observation that the processed form of AtSerpin1 can be detected in the RD21-ko line indicates that a complex-independent pathway for AtSerpin1 processing exists that is likely mediated by other proteases.

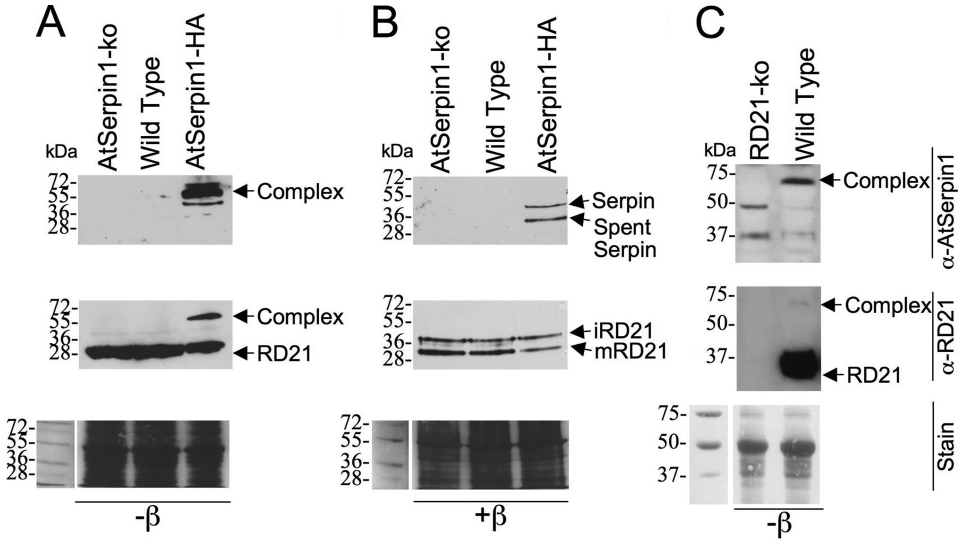

FIGURE 5. **Detection of RD21 as part of a complex with AtSerpin1.** Extracts (200 μg) from 2-week-old plants were fractionated on reducing (+β) or nonreducing gels (−β) as described under "Experimental Procedures," and the immunoblots were developed with different antibodies as indicated. *A*, immunoblot of AtSerpin1-ko, wild type, and AtSerpin1-HA extracts fractionated by nonreducing SDS-PAGE and immunoblotted with α-AtSerpin1 (*upper panel*) or α-RD21 (*lower panel*). *B*, extracts as in *A* were fractionated by reducing SDS-PAGE. *C*, immunoblot of wild type and RD21-ko extracts (120 μg) fractionated in nonreducing gel and immunoblotted with α-AtSerpin1 (*upper panel*) or α-RD21 (*middle panel*). The *lower panels* are loading controls and stained markers.

In Vitro Generation of AtSerpin1 Complex—Generation of stable protease-serpin complex from the native stressed form of a serpin requires specific cleavage of the reactive center by its cognate protease. To examine if this interaction can be reconstructed *in vitro*, recombinant His-AtSerpin1 was added to extracts of AtSerpin1-ko and RD21-ko plants. As shown in Fig. 6*A*, RD21 was present in the fast migrating form in the AtSerpin1-ko extracts and was absent in RD21-ko

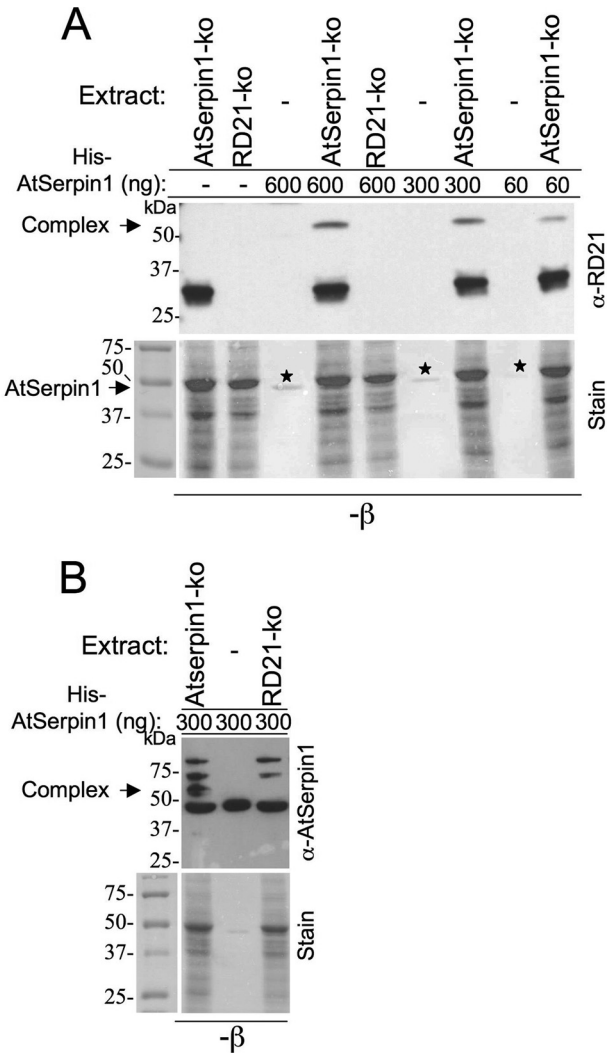

FIGURE 6. **Recombinant His-AtSerpin1 forms a complex with RD21 *in vitro*.** Recombinant His-AtSerpin1 was incubated with extracts from 2-week-old leaves of the following lines: AtSerpin1-ko, RD21-ko prepared in binding buffer, or incubated with binding buffer alone (−). The mixtures were then fractionated by nonreducing SDS-PAGE as described under "Experimental Procedures," and the immunoblots were processed with antibody α-RD21 or α-AtSerpin1 as indicated. The Coomassie stain is shown *below* the immunoblots. *A,* recombinant His-AtSerpin1 (60, 300, or 600 ng) was incubated with or without extracts (120 μg) in a 30-μl final volume for 30 min, and the immunoblot was developed with RD21 antibody. *Asterisks* indicate position of recombinant His-AtSerpin1. *B,* recombinant His-AtSerpin1 protein (300 ng) was incubated with or without extracts from mutant leaves (120 μg) in a 30-μl final volume for 10 min. The immunoblot was developed with AtSerpin1 antibody.

extracts (as anticipated). However, upon addition of recombinant His-AtSerpin1 to AtSerpin1-ko, but not to RD21-ko extracts, RD21 migrated as a complex (Fig. 6*A*). The amount of complex observed was sensitive to the amount of recombinant His-AtSerpin1 added. When recombinant His-AtSerpin1 was added to AtSerpin1-ko extracts and immunoblotted with α-AtSerpin1, the expected serpin-RD21 complex size was detected (*arrow*, Fig. 6*B*) as well as slower migrating forms. When recombinant His-AtSerpin1 was added to RD21-ko extracts, the AtSerpin1-RD21 complex was not detected; however, both slower migrating forms remained. The slower migrating bands could represent AtSerpin1 dimers or *in vitro* interaction with noncognate proteases. The results demonstrate that RD21 can interact with AtSerpin1 *in vitro* to form stable migrating complexes.

DISCUSSION

AtSerpin1 Shows Commonalities and Differences with Known Serpin Structures—The structure of AtSerpin1 is the first for a plant serpin and illustrates features that are specific for this protein and other features that likely characterize the majority of plant serpins. Plant serpin sequences are observed to contain a plant-specific insertion between s2B and s3B, including a motif specific to plant serpins. The conserved Asp-230 and Arg-232 residues in this motif form a hydrogen-bonded structure that stabilizes the loop between hD and s2A. This area is disordered in many serpin structures, and we postulate that in plant serpins this region will be stabilized. This stabilization may contribute to the fact that the breach (between s3A and s5A in β-sheet sA) in AtSerpin1 is unusually open when compared with non-plant stressed state serpin structures (Fig. 1, *E* and *F*). It is possible that the ordering of the loop between hD and s2A contributes to holding the breach in a more open conformation. Indeed, the open structure resembles other serpin structures where the RCL has partially inserted into β-sheet sA (5).

An enlarged breach region has been shown to play important roles in serpin biology. For example, the spontaneously polymerizing Z-mutant of α_1-antitrypsin accumulates as polymers in hepatocytes causing juvenile hepatitis, cirrhosis, and hepatocellular carcinoma (54). Z-α_1-antitrypsin differs from the wild type inhibitor by a single substitution E342K in the breach region. The mutation disrupts a salt bridge and induces molecular perturbations that may facilitate opening of β-sheet A, resulting in a structure that is prone to polymerize (54). An open breach is in contrast to that seen in Maspin (SERPINB5) where the bonding pattern of the region between s3A and s5A is essentially complete, consistent with the complete absence of a loop insertion process in that serpin (55). Notwithstanding the more open breach, higher order AtSerpin1 structures were not observed in nondenaturing gel fractionation of plant extracts.

The charge distribution at the "top" of AtSerpin1 (β-sheet sC) is unusual (Fig. 1, *B* and *D*). The molecule also features a unique distribution of charges in its RCL, which differs from those of other *Arabidopsis* serpins. In addition, the surface of sC is highly positively charged lying beneath the RCL, which is also positively charged between P14 and P4′. It is possible that the natural target protease includes in its active site residues that accommodate the serpin-positive charge. Surface electrostatic interactions have been found to play a role in substrate binding of polyanions, for example, in the activation of the serpin heparin cofactor II by heparin (reviewed in Ref. 56). The presence of special charge features in the AtSerpin1 RCL and the more open breach are consistent with those regions tending to show the most conformational plasticity when examining the complete spectrum of serpin structures (2). Our evidence shows that AtSerpin1 is present in the secretory pathway, and a potential glycosylation site is present near the C terminus of AtSerpin1 (Asn-375). Potential glycosylation sites have been found in other plant serpins (12). However, this site in AtSerpin1 is not conserved in plant serpins, with the majority having either

aspartic acid or glutamic acid in place of the asparagine (60/67 expressed plant serpin sequences). The site is situated on the surface of the protein in the loop between strands s4B and s5B, and if glycosylated it would likely not influence overall serpin structure.

AtSerpin1 Interaction with RD21—AtSerpin1 is shown here to interact with the cysteine protease RD21. The formation of complex is dependent in the presence of both the specific serpin and on RD21 as the complex is not detected in knock-out mutants. The amount of complex is enhanced in the presence of AtSerpin1 overexpression. However, the overexpression itself does not seem to otherwise change the total amount of detectable protease but rather its distribution between the free and complex-bound forms. AtSerpin1 is predicted to belong to a subgroup of plant serpins that contain a secretory motif in the N terminus (supplemental Fig. S2). Indeed, AtSerpin1 is found secreted in root exudates as a processed 28-kDa form (Fig. 2*F*). The origin of this form is unknown, although N-terminal processing of other serpins like α-antitrypsin by human mesotrypsin has been reported previously (57). AtSerpin1 was detected immunologically by electron microscopy in the ER and Golgi (18). Its target protease, RD21, is also targeted to the secretary system. It has been detected in vacuoles (25) and special protease storing bodies derived from the ER (58). The results here imply that AtSerpin1 and RD21 interact in either one or in both of these subcellular compartments.

AtSerpin1 has been shown to interact *in vitro* with the metacaspase AtMC9 to yield a stable complex; however, no *in vivo* interactions were reported (18). AtMC9 is part of a unique clan of cysteine proteases and is of unknown function (59). The preferred residue of AtMC9 for cleavage is at Arg-351 at the canonical P1 position of AtSerpin1. Proteolysis at this site would yield a serpin N-terminal residual fragment of 38 kDa, which is consistent with the size range of the processed serpin detected here. However, our data show that AtSerpin1 can interact *in vivo* to form an E-64-sensitive complex implicating the involvement of papain-like cysteine protease activity. Although AtSerpin1 was shown to interact *in vitro* with AtMC9, the latter is insensitive to E-64 (60). We have observed SDS-stable AtSerpin1-trypsin complexes *in vitro* (data not shown). Indeed, some serpins show a high degree of promiscuity in their ability to form complexes with very divergent proteases (2). Although our results, substantiated by direct immunodetection and mutant analysis, implicated only AtSerpin1-RD21 interaction at the particular developmental stages examined, they do not rule out the potential participation of other protease targets, including AtMC9. Indeed, processing of the AtSerpin1 protein is detected in the RD21-ko line indicating that other target proteases with the ability to cleave AtSerpin1 may exist, but they do not form stable complexes.

Leaf tissue vacuolar processing cysteine-type enzymes (VPE) accumulate in bodies directly derived from the ER. These bodies represent ER and Golgi complexes that play a role in vacuolar transport under stress conditions (61–63). VPE proteases are involved in the hypersensitive response to viral infection (64), and VPE-null mutants showed reduced mycotoxin-induced vacuolar membrane damage (65). However, VPE proteases, which were reported to be involved in the induction of cell death, are not inhibited by E-64 (65). Based on this evidence, it is unlikely that AtMC9 or VPE-type proteases are the source of the *in vivo* complex detected here; however, a plethora of other cysteine proteases exists as candidate AtSerpin1 targets. Cysteine proteases have been shown to be associated with general stress effects (20, 22, 23). Importantly, AtSerpin1 is an example of the "LR serpins," which have P2-P1′ Leu-Arg-Xaa (where Xaa is a small residue) in the reactive center. Thus, the highly conserved serpin reactive center Leu-Arg-Xaa present in many diverse plant species, along with conserved features of RD21, suggest that the function of AtSerpin1 and its cognate proteases may be conserved across the plant kingdom (9). In this respect, it is of interest that RD21 homologues are prevalent in many plant species. In maize, an RD21 homologue (cysteine protease of protease-inhibitor complex) is found in seeds as a complex with the small cysteine protease inhibitor, cystatin (66), whereas the rice RD21 homologue appears to be induced in leaves during UV radiation and fungal infection (67).

RD21 is synthesized as a preproprotein that is proteolytically processed to a mature active form. In *Arabidopsis*, RD21 accumulates as a stress-inducible protease in protease-storing bodies of epidermal cells (58). The two main forms that accumulate are the mature mRD21, which contains the core mature protease, and the immature iRD21 form, which contains a granulin-like C-terminal extension. In this case, the acidic environment of the vacuole is thought to play a role in maturation (25). Intriguingly, the highly conserved granulin domain in animals acts as a mitogen for epithelial and fibroblastic cells (68) and promotes cell division (69). Although accessory proteases are thought to play a role in RD21 processing, vacuolar processing enzyme-γ (VPEγ) is not involved (70). It is intriguing to consider what role, if any, the association of RD21 with AtSerpin1 may have in this processing.

Although our results demonstrate the presence of an endogenous plant protease target, it remains possible that AtSerpin1 also plays a role in direct inhibition of microbial or insect proteases as suggested for the highly abundant serpins in seeds (71). Interestingly, in developing seeds, an ER resident protein, PDI5 (protein-disulfide isomerase 5), was detected by yeast two-hybrid screens and by *in vitro* inhibition of protease activity to interact with RD21 (62). The authors suggested that PDI5 plays a role in modifying protease trafficking and activity before programmed cell death of seed endothelium cells. Why RD21 has been targeted for control at multiple developmental nexus, *i.e.* seeds and leaves, is not known, but in addition to containing a unique granulin domain, RD21 exhibits a peculiar enzymatic trait, it accepts peptides and ligates them to the N termini of acceptor proteins (53). Thus, it is possible that AtSerpin1 functions to curb this activity.

The discovery that AtSerpin1 is the *in vivo* serpin inhibitor of RD21 will provide a new and powerful tool for investigating the regulation of programmed cell death-dependent processes. Our results present a conceptual and experimental framework for analysis of serpins and their protease targets in plants. Further work will clarify the functionally conserved and unique aspects of serpin-dependent regulation of signaling protease cascades in plant biology.

Acknowledgments—We thank Dr. Mika Jormakka at the Centenary Institute of Cancer Medicine and Cell Biology at the University of Sydney, Australia, for x-ray data collection at the synchrotron at the Argonne National Laboratory, Chicago. GM/CA-CAT has been funded in whole or in part by National Institutes of Health Grant Y1-CO-1020 from NCI and Grant Y1-GM-1104 from NIGMS. Use of the Advanced Photon Source was supported by the United States Department of Energy, Basic Energy Sciences, Office of Science, under Contract DE-AC02-06CH11357. We thank Dr. Galia Blum and Prof. Matthew Bogyo, Stanford University, for kindly providing DCG-04 probe. We thank Prof. Ikuko Hara-Nishimura, Kyoto University, for kindly providing RD21 antibody and Dr. Renier A. L. van der Hoorn, Max Planck Institute for Plant Breeding Research, for kindly providing the RD21-ko line.

REFERENCES

1. Levashina, E. A., Langley, E., Green, C., Gubb, D., Ashburner, M., Hoffmann, J. A., and Reichhart, J. M. (1999) *Science* **285,** 1917–1919
2. Huntington, J. A. (2006) *Trends Biochem. Sci.* **31,** 427–435
3. Schechter, I., and Berger, A. (1967) *Biochem. Biophys. Res. Commun.* **27,** 157–162
4. Huntington, J. A., Read, R. J., and Carrell, R. W. (2000) *Nature* **407,** 923–926
5. Gettins, P. G. (2002) *Chem. Rev.* **102,** 4751–4804
6. Janciauskiene, S. (2001) *Biochim. Biophys. Acta* **1535,** 221–235
7. Law, R. H., Zhang, Q., McGowan, S., Buckle, A. M., Silverman, G. A., Wong, W., Rosado, C. J., Langendorf, C. G., Pike, R. N., Bird, P. I., and Whisstock, J. C. (2006) *Genome Biol.* **7,** 216
8. Nielsen, H. M., Minthon, L., Londos, E., Blennow, K., Miranda, E., Perez, J., Crowther, D. C., Lomas, D. A., and Janciauskiene, S. M. (2007) *Neurology* **69,** 1569–1579
9. Roberts, T. H., and Hejgaard, J. (2008) *Funct. Integr. Genomics* **8,** 1–27
10. Dahl, S. W., Rasmussen, S. K., and Hejgaard, J. (1996) *J. Biol. Chem.* **271,** 25083–25088
11. Hejgaard, J., and Hauge, S. (2002) *Physiol. Plant* **116,** 155–163
12. Ostergaard, H., Rasmussen, S. K., Roberts, T. H., and Hejgaard, J. (2000) *J. Biol. Chem.* **275,** 33272–33279
13. Hejgaard, J. (2001) *FEBS Lett.* **488,** 149–153
14. Roberts, T. H., Marttila, S., Rasmussen, S. K., and Hejgaard, J. (2003) *J. Exp. Bot.* **54,** 2251–2263
15. la Cour Petersen, M., Hejgaard, J., Thompson, G. A., and Schulz, A. (2005) *J. Exp. Bot.* **56,** 3111–3120
16. Kehr, J. (2006) *J. Exp. Bot.* **57,** 767–774
17. Yoo, B. C., Aoki, K., Xiang, Y., Campbell, L. R., Hull, R. J., Xoconostle-Cázares, B., Monzer, J., Lee, J. Y., Ullman, D. E., and Lucas, W. J. (2000) *J. Biol. Chem.* **275,** 35122–35128
18. Vercammen, D., Belenghi, B., van de Cotte, B., Beunens, T., Gavigan, J. A., De Rycke, R., Brackenier, A., Inzé, D., Harris, J. L., and Van Breusegem, F. (2006) *J. Mol. Biol.* **364,** 625–636
19. Ahn, J. W., Atwell, B. J., and Roberts, T. H. (2009) *BMC Plant Biol.* **9,** 52
20. Schaller, A. (2004) *Planta* **220,** 183–197
21. Piszczek, E., and Gutman, W. (2007) *Acta Physiol. Plant* **29,** 391–398
22. Bonneau, L., Ge, Y., Drury, G. E., and Gallois, P. (2008) *J. Exp. Bot.* **59,** 491–499
23. Grudkowska, M., and Zagdańska, B. (2004) *Acta Biochim. Pol.* **51,** 609–624
24. Kinoshita, T., Yamada, K., Hiraiwa, N., Kondo, M., Nishimura, M., and Hara-Nishimura, I. (1999) *Plant J.* **19,** 43–53
25. Yamada, K., Matsushima, R., Nishimura, M., and Hara-Nishimura, I. (2001) *Plant Physiol.* **127,** 1626–1634
26. Bozhkov, P. V., Filonova, L. H., Suarez, M. F., Helmersson, A., Smertenko, A. P., Zhivotovsky, B., and von Arnold, S. (2004) *Cell Death Differ.* **11,** 175–182
27. Solomon, M., Belenghi, B., Delledonne, M., Menachem, E., and Levine, A. (1999) *Plant Cell* **11,** 431–444
28. Belenghi, B., Acconcia, F., Trovato, M., Perazzolli, M., Bocedi, A., Polticelli, F., Ascenzi, P., and Delledonne, M. (2003) *Eur. J. Biochem.* **270,** 2593–2604
29. Watanabe, N., and Lam, E. (2005) *J. Biol. Chem.* **280,** 14691–14699
30. Bosch, M., and Franklin-Tong, V. E. (2007) *Proc. Natl. Acad. Sci. U.S.A.* **104,** 18327–18332
31. He, R., Drury, G. E., Rotari, V. I., Gordon, A., Willer, M., Farzaneh, T., Woltering, E. J., and Gallois, P. (2008) *J. Biol. Chem.* **283,** 774–783
32. del Pozo, O., and Lam, E. (1998) *Curr. Biol.* **8,** 1129–1132
33. Elbaz, M., Avni, A., and Weil, M. (2002) *Cell Death Differ.* **9,** 726–733
34. Chichkova, N. V., Kim, S. H., Titova, E. S., Kalkum, M., Morozov, V. S., Rubtsov, Y. P., Kalinina, N. O., Taliansky, M. E., and Vartapetian, A. B. (2004) *Plant Cell* **16,** 157–171
35. Gettins, P. G., and Olson, S. T. (2009) *J. Biol. Chem.* **284,** 20441–20445
36. Irving, J. A., Pike, R. N., Lesk, A. M., and Whisstock, J. C. (2000) *Genome Res.* **10,** 1845–1864
37. van Gent, D., Sharp, P., Morgan, K., and Kalsheker, N. (2003) *Int. J. Biochem. Cell Biol.* **35,** 1536–1547
38. Harp, J. M., Timm, D. E., and Bunick, G. J. (1998) *Acta Crystallogr. D Biol. Crystallogr.* **54,** 622–628
39. CCP4 (1994) *Acta Crystallogr. D Biol. Crystallogr.* **50,** 760–763
40. McCoy, A. J., Grosse-Kunstleve, R. W., Adams, P. D., Winn, M. D., Storoni, L. C., and Read, R. J. (2007) *J. Appl. Crystallogr.* **40,** 658–674
41. Harrop, S. J., Jankova, L., Coles, M., Jardine, D., Whittaker, J. S., Gould, A. R., Meister, A., King, G. C., Mabbutt, B. C., and Curmi, P. M. (1999) *Structure* **7,** 43–54
42. Emsley, P., and Cowtan, K. (2004) *Acta Crystallogr. D Biol. Crystallogr.* **60,** 2126–2132
43. Adams, P. D., Grosse-Kunstleve, R. W., Hung, L. W., Ioerger, T. R., McCoy, A. J., Moriarty, N. W., Read, R. J., Sacchettini, J. C., Sauter, N. K., and Terwilliger, T. C. (2002) *Acta Crystallogr. D Biol. Crystallogr.* **58,** 1948–1954
44. Fass, E., Shahar, S., Zhao, J., Zemach, A., Avivi, Y., and Grafi, G. (2002) *J. Biol. Chem.* **277,** 30921–30927
45. Alonso, J. M., Stepanova, A. N., Leisse, T. J., Kim, C. J., Chen, H., Shinn, P., Stevenson, D. K., Zimmerman, J., Barajas, P., Cheuk, R., Gadrinab, C., Heller, C., Jeske, A., Koesema, E., Meyers, C. C., Parker, H., Prednis, L., Ansari, Y., Choy, N., Deen, H., Geralt, M., Hazari, N., Hom, E., Karnes, M., Mulholland, C., Ndubaku, R., Schmidt, I., Guzman, P., Aguilar-Henonin, L., Schmid, M., Weigel, D., Carter, D. E., Marchand, T., Risseeuw, E., Brogden, D., Zeko, A., Crosby, W. L., Berry, C. C., and Ecker, J. R. (2003) *Science* **301,** 653–657
46. Finn, R. D., Tate, J., Mistry, J., Coggill, P. C., Sammut, S. J., Hotz, H. R., Ceric, G., Forslund, K., Eddy, S. R., Sonnhammer, E. L., and Bateman, A. (2008) *Nucleic Acids Res.* **36,** D281–D288
47. Chuang, Y. J., Gettins, P. G., and Olson, S. T. (1999) *J. Biol. Chem.* **274,** 28142–28149
48. Simonovic, I., and Patston, P. A. (2000) *Biochim. Biophys. Acta* **1481,** 97–102
49. Schick, C., Kamachi, Y., Bartuski, A. J., Cataltepe, S., Schechter, N. M., Pemberton, P. A., and Silverman, G. A. (1997) *J. Biol. Chem.* **272,** 1849–1855
50. Barrett, A. J., Kembhavi, A. A., Brown, M. A., Kirschke, H., Knight, C. G., Tamai, M., and Hanada, K. (1982) *Biochem. J.* **201,** 189–198
51. Greenbaum, D., Baruch, A., Hayrapetian, L., Darula, Z., Burlingame, A., Medzihradszky, K. F., and Bogyo, M. (2002) *Mol. Cell. Proteomics* **1,** 60–68
52. van der Hoorn, R. A., Leeuwenburgh, M. A., Bogyo, M., Joosten, M. H., and Peck, S. C. (2004) *Plant Physiol.* **135,** 1170–1178
53. Wang, Z., Gu, C., Colby, T., Shindo, T., Balamurugan, R., Waldmann, H., Kaiser, M., and van der Hoorn, R. A. (2008) *Nat. Chem. Biol.* **4,** 557–563
54. Lomas, D. A., Evans, D. L., Finch, J. T., and Carrell, R. W. (1992) *Nature* **357,** 605–607
55. Al-Ayyoubi, M., Gettins, P. G., and Volz, K. (2004) *J. Biol. Chem.* **279,** 55540–55544
56. Patston, P. A., Church, F. C., and Olson, S. T. (2004) *Methods* **32,** 93–109
57. Szepessy, E., and Sahin-Tóth, M. (2006) *FEBS J.* **273,** 2942–2954

58. Hayashi, Y., Yamada, K., Shimada, T., Matsushima, R., Nishizawa, N. K., Nishimura, M., and Hara-Nishimura, I. (2001) *Plant Cell Physiol.* **42,** 894–899
59. Vercammen, D., Declercq, W., Vandenabeele, P., and Van Breusegem, F. (2007) *J. Cell Biol.* **179,** 375–380
60. Vercammen, D., van de Cotte, B., De Jaeger, G., Eeckhout, D., Casteels, P., Vandepoele, K., Vandenberghe, I., Van Beeumen, J., Inzé, D., and Van Breusegem, F. (2004) *J. Biol. Chem.* **279,** 45329–45336
61. Gruis, D. F., Selinger, D. A., Curran, J. M., and Jung, R. (2002) *Plant Cell* **14,** 2863–2882
62. Andème Ondzighi, C., Christopher, D. A., Cho, E. J., Chang, S. C., and Staehelin, L. A. (2008) *Plant Cell* **20,** 2205–2220
63. Otegui, M. S., Herder, R., Schulze, J., Jung, R., and Staehelin, L. A. (2006) *Plant Cell* **18,** 2567–2581
64. Hatsugai, N., Kuroyanagi, M., Yamada, K., Meshi, T., Tsuda, S., Kondo, M., Nishimura, M., and Hara-Nishimura, I. (2004) *Science* **305,** 855–858
65. Kuroyanagi, M., Yamada, K., Hatsugai, N., Kondo, M., Nishimura, M., and Hara-Nishimura, I. (2005) *J. Biol. Chem.* **280,** 32914–32920
66. Yamada, T., Ohta, H., Shinohara, A., Iwamatsu, A., Shimada, H., Tsuchiya, T., Masuda, T., and Takamiya, K. (2000) *Plant Cell Physiol.* **41,** 185–191
67. Fu, Y., Zhao, W., and Peng, Y. (2007) *J. Plant Res.* **120,** 465–469
68. Zhou, J., Gao, G., Crabb, J. W., and Serrero, G. (1993) *J. Biol. Chem.* **268,** 10863–10869
69. Zhang, H., and Serrero, G. (1998) *Proc. Natl. Acad. Sci. U.S.A.* **95,** 14202–14207
70. Rojo, E., Zouhar, J., Carter, C., Kovaleva, V., and Raikhel, N. V. (2003) *Proc. Natl. Acad. Sci. U.S.A.* **100,** 7389–7394
71. Hejgaard, J., and Roberts, T. H. (2007) in *Molecular and Cellular Aspects of the Serpinopathies and Disorders in Serpin Activity* (Silverman, G. A., and Lomas, D. A., eds) pp. 279–300, World Scientific Publishing Co., Hackensack, NJ